Polymer 49 (2008) 3310–3317

Contents lists available at ScienceDirect

Polymer

journal homepage: www.elsevier.com/locate/polymer

Cure behavior of epoxy/MWCNT nanocomposites: The effect of nanotube surface modification

Mohamed Abdalla [a], Derrick Dean [a,*], Pamela Robinson [b], Elijah Nyairo [c]

[a] The University of Alabama at Birmingham, Department of Materials Science and Engineering, 1530 3rd Avenue South, Birmingham, AL 35294-4461, USA
[b] Tuskegee University, Department of Chemistry, Tuskegee, AL 36088, USA
[c] Alabama State University, Department of Physical Science, Montgomery, AL 36101, USA

ARTICLE INFO

Article history:
Received 13 February 2008
Received in revised form 28 April 2008
Accepted 3 May 2008
Available online 16 May 2008

Keywords:
Carbon nanotubes
Epoxy nanocomposite
Cure kinetics

ABSTRACT

The effect of carboxyl and fluorine modified multi-wall carbon nanotubes (MWCNTs) on the curing behavior of diglycidyl ether of bisphenol A (DGEBA) epoxy resin was studied using differential scanning calorimetry (DSC), rheology and infrared spectroscopy (IR). Activation energy (E_a) and rate constants (k) obtained from isothermal DSC were the same for the neat resin and fluorinated MWCNT system (47.7 and 47.5 kJ/mol, respectively) whereas samples containing carboxylated MWCNTs exhibited a higher activation energy (61.7 kJ/mol) and lower rate constant. Comparison of the activation energies, rate constants, gelation behavior and vitrification times for all of the samples suggests that the cure mechanisms of the neat resin and fluorinated sample are similar but different from the carboxylated sample. This can be explained by the difference in how the fluorinated nanotubes react with the epoxy resin compared to the carboxylated nanotubes. Although the two systems have different reaction mechanisms, both systems have similar degrees of conversion as calculated from the infrared spectroscopic data, glass transition temperature (T_g), and predictions based on DSC data. This difference in reaction mechanism may be attributed to differences in nanotube dispersion; the fluorinated MWCNT system is more uniformly dispersed in the matrix whereas the more heterogeneously dispersed carboxylated MWCNTs can hinder mobility of the reactive species and disrupt the reaction stoichiometry on the local scale.

1. Introduction

Since the discovery of carbon nanotubes (CNTs) in 1991, they have inspired scientists to consider them for a range of potential applications and have become one of the most promising fillers for reinforcement of multi-functional nanocomposites [1–4]. In particular, the use of CNTs in polymer nanocomposites has attracted wide attention due to their excellent mechanical, electrical, and thermal properties. CNTs have a unique atomic structure and can achieve very high aspect ratios since their diameters are in the range of a few nanometers with lengths of several hundred nanometers. CNTs also have extraordinary mechanical properties. Individually, CNTs have Young's moduli ranging from 270 GPa to 2 TPa and tensile strength from 11 to 200 GPa making them ideal as reinforcing fillers for nanocomposites [4–12].

In light of these exceptional properties, CNTs are dispersed in a wide range of matrices including polymers, ceramics, resins, metals and other matrices to enhance the mechanical, electronic, and thermal properties of the resulting nanocomposites. Epoxy resins are one of the most important thermoset polymers and have been used extensively because of their performance. Using CNTs as reinforcement in epoxy nanocomposites can widen their use in potential applications such as coatings, adhesives, potting compounds, encapsulates, structural materials, liquid crystal display, etc. [7,13–15].

Many studies have shown considerable property enhancement in CNT/epoxy nanocomposites [12,16–28]. For example, dispersing 0.2–10 wt% CNTs into epoxy resins results in modulus enhancements up to 50% [14] and strength enhancements up to 18% [28]. However, these property enhancements are far below the expected improvements based on the properties of the CNTs. Several studies have suggested that the properties can be improved even further if better dispersions and more efficient load transfer can be achieved [1,5,9,18,23,27,29–34]. One of the most promising approaches designed to address this issue involves chemically modifying the nanotube surface before dispersing it into the prepolymer.

Several recent studies have verified that excellent dispersions of CNTs in epoxy resins can be achieved by chemically modifying the nanotube surfaces [2,9,35]. However, the modulus and strength enhancements achieved were similar to those reported earlier for epoxies dispersed with unmodified CNTs. Clearly, CNTs' modification enhances dispersion and the resulting properties. It is not clear,

* Corresponding author.
E-mail address: deand@uab.edu (D. Dean).

0032-3861/$ – see front matter © 2008 Elsevier Ltd. All rights reserved.
doi:10.1016/j.polymer.2008.05.016

however, how the modified CNTs react with the epoxy resins and how this affects the final properties. The differences in the way the epoxy and/or the amine curing agent reacts with the different nanotube modifications can result in steric and electronic differences that can, in turn, affect the cure. This should be evident in variations in the cure behavior. Thus studying the curing behavior of the CNT/epoxy nanocomposites is very important for understanding and optimizing the processing conditions and ultimate properties.

Several recent studies have investigated the cure kinetics of CNT/epoxy systems [18,22,23,36–38]. For example, Kenny et al. used Raman spectroscopy and thermal analysis to investigate the effect of incorporating *unmodified* single wall carbon nanotubes (SWCNTs) on the cure reaction of a diglycidyl ether of bisphenol A (DGEBA) resin [38]. They observed a shift in the DSC exothermic reaction peak to lower temperatures when SWNTs were added and attributed this to a catalytic effect caused by the high thermal conductivity of the CNTs. This finding was further correlated with the morphology, which was studied using Raman spectroscopy. They found that the epoxy expanded the spacing between the CNTs. The increased surface area was presumed to contribute to the higher thermal conductivity.

Tao et al. used DSC to study the effect of CNT types on the cure behavior of a DGEBA epoxy cured with Epicure W [39]. All of the CNTs were SWNTs with *no surface modification*. From dynamic DSC studies, they found that all SWNTs initiated curing at a lower temperature relative to the neat resin, while the overall degree of cure was lower. Isothermal DSC studies only showed discernable differences in cure behavior during the early stages (first 20 min) of cure.

Review of the studies cited above shows that very few efforts have been made to address the influence of *modified* CNTs on the cure behavior of the epoxy system, thus the study of cure kinetics remains an area of interest. In this work, we examine the cure reaction of diglycidyl ether of bisphenol A-based epoxy resin (EPON828) dispersed with two different *modified* multi-wall CNTs (carboxylic acid and fluorinated). The curing behavior of CNT/EPON828 was evaluated by *quasi-isothermal* modulated differential scanning calorimetry (MDSC), Fourier-transform infrared (FT-IR) spectroscopy and rheology. The findings are correlated with the differences in CNTs' surface chemistry.

2. Experimental

2.1. Materials

The EPIKOTE resin, EPON828, and Epicure curing agent, W, were purchased from Miller–Stephenson Company. EPON828 is diglycidyl ether of bisphenol A (DGEBA) and W is a non-methylene dianiline, aromatic amine curing agent (diethyltoluenediamine). Their chemical structures are shown in Fig. 1. The MWCNTs were purchased from Materials and Electrochemical Research (MER) Corporation and used as-received. The MWCNTs were synthesized by catalytic chemical vapor deposition (CVD) with 35 nm diameter and approximately 30 μm length. The purity of as-received MWCNT was greater than 90%, with less than 0.1% metal (Fe) content.

2.2. Epoxy/MWCNT synthesis

2.2.1. Chemical treatment

2.2.1.1. Carboxylation of carbon nanotubes. The CNTs were treated with a mixture of sulfuric/nitric acid, which helped to remove impurities from the surface. A 1 g portion of CNTs was added to a mixture of sulfuric/nitric acid (3:1 by volume, respectively). The mixture was sonicated in a water bath for 3 h at 40 °C. The mixture was then diluted to 1:5, by volume of acid/water, with distilled water. The CNTs were recovered by filtering the mixture through polycarbonate membrane filter (ATTP 0.8 μm pore size) and washed with an excess of water until no residual acid was present. Finally, the CNTs were dried for 24 h in a vacuum oven. This resulted in –COOH groups on the surface. These modified CNTs are designated COOH–MWCNT.

2.2.1.2. Fluorination of carbon nanotubes. In a flame-dried three-necked round-bottom flask fitted with a condenser a 1 g of MWCNT, 15 mL of 2-methoxyethyl ether, and 3.1 mL of 4-fluoroaniline were added. The mixture was purged by bubbling nitrogen through a needle. While maintaining an inert atmosphere 4 mL of amyl nitrate was added slowly using a dropping funnel. The mixture was stirred at room temperature for 1 h and then the temperature was raised to 70 °C and the mixing was continued for 3 h. The product was cooled, diluted with diethyl ether, filtered and then washed with copious amounts of water. The wet product was dried in vacuum oven for 24 h. This modified CNTs are designated F–MWCNT.

2.2.2. Sample preparation

An appropriate amount of MWCNT to prepare 1% CNT samples was dispersed into the epoxy resin by using an extrusion process. Using two syringes, the mixture was extruded from one syringe into the other syringe with the help of pneumatic device. This process was repeated up to 50 times to ensure a good dispersion. Then the equivalent amount of curing agent was added and mixed using the same process. Several DSC aluminum pans were filled with the reaction mixture. The samples (ca. 10 mg) were stored in a freezer until tested. These samples are designated as COOH–MWNT/EPON and F–MWNT/EPON for the carboxylated and fluorinated systems, respectively.

2.3. Characterization

2.3.1. DSC

Thermal characterization was performed using a Q100 DSC (TA Instruments Inc, Delaware). The curing processes of the epoxy were studied using isothermal scans on 10 mg samples. Quasi-isothermal scans were conducted in the modulated DSC (MDSC) mode. In this mode each sample was ramped from room temperature to the desired isothermal temperature and then held isothermally. The temperature was then modulated using amplitude of ±0.50 °C every 60 s for 240 min. The isothermal experiments were conducted at three temperatures (110, 122, and 140 °C). The total area under the exotherm curve was used to calculate the heat of reaction at each temperature. Cured samples were also tested with DSC to determine the glass transition temperatures using a dynamic procedure; 10 mg of cured samples were heated from room temperature to 350 °C at a heating rate of 10 °C/min. All DSC scans were conducted using hermetically sealed aluminum sample pans and 50 mL/min of N_2 purge. Exothermic peaks are represented by upward peaks in the DSC thermograms. The kinetic analysis was done using TA Advantage Specialty Library package provided by TA instruments.

2.3.2. IR

Infrared spectra were recorded on a Nicolet 4700 Fourier-transform infrared (FT-IR) spectrometer using a heated attenuated total reflection (ATR). IR spectra were obtained using a resolution of 4.0 $cm^{-1}$and 32 scans.

2.3.3. Rheology

Rheological experiments were conducted on an AR2000 rheometer (TA Instruments Inc, Delaware), in rate control mode, using

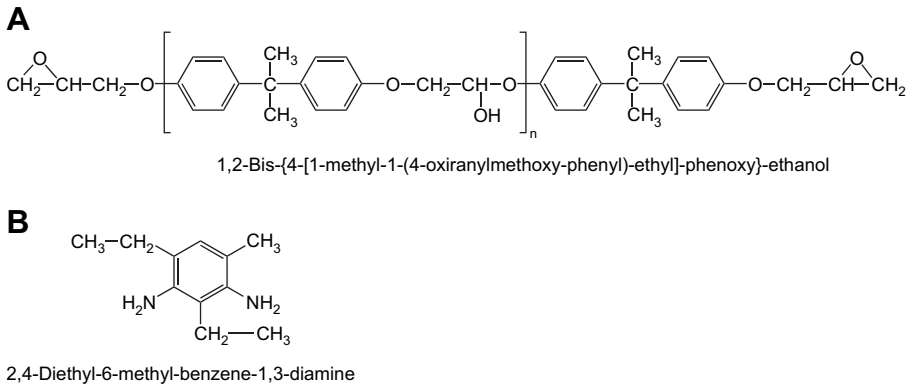

Fig. 1. Chemical structure of (A) EPON828 and (B) Epicure W.

a parallel plate geometry. Isothermal time sweeps were conducted at 122 °C using a gap of 1 mm and a strain of 1%.

3. Results and discussion

3.1. Isothermal DSC measurements of curing process

Isothermal curing studies were conducted in order to determine the kinetic parameters for the curing reaction. In general, the curing kinetics of epoxy resins can be categorized as *n*-th order or autocatalyzed. The *n*-th order reaction was originally described by Borchardt and Daniels [40] for solutions and was subsequently refined for solids [41]. It permits the calculation of activation energy (E_a), pre-exponential factor (Z), heat of reaction (ΔH), reaction order (n), and rate constant (k) from a single DSC scan. The approach assumes that the reaction obeys the general rate equation:

$$\frac{d\alpha}{dt} = k(T)(1-\alpha)^n \quad (1)$$

where $d\alpha/dt$ = reaction rate (1/s), α = fractional conversion, $k(T)$ = specific rate constant at temperature T and n = reaction order. The approach also assumes Arrhenius behavior:

$$k(T) = Ze^{-E_a/RT} \quad (2)$$

where E_a = Activation energy (J/mol), Z = pre-exponential factor (1/sec), R = gas constant = 8.314 J/mol K.

Reactions obeying the *n*-th order kinetics will exhibit a maximum reaction rate at time $t = 0$, while an autocatalyzed reaction exhibits a maximum reaction rate at 30–40% of the reaction and the formation of intermediate species which initiate and accelerate the reaction [40–45]. The epoxy system used in this study clearly follows autocatalyzed cure kinetics, as shown in Fig. 2 which shows heat flow vs. time (t) at 120 °C for the neat resin and 1% COOH–MWCNT/EPON828 and F–MWCNT/EPON828 nanocomposites.

The peak onset time and the corresponding enthalpic change at the three isothermal temperatures used in this study are reported in Table 1. In general, the values of the isothermal ΔH increase as isothermal cure temperature increases. This is caused by the fact that the increase in isothermal reaction temperature for exothermic reactions generates heat in a higher proportion than the heat generated by the reaction itself. For a given reaction temperature, the ΔH decreases and the peak onset time increases relative to the neat resin. This suggests that the reactions are being affected by the presence of the nanotubes. The opposite effect was observed by Kenny et al., i.e. for a given temperature, the peak onset time decreases with CNT addition, for a DGEBA/SWNT nanocomposite [37,46]. The difference may stem from the fact that modified carbon nanotubes are used in our study.

The data reported in Table 1 was analyzed using the autocatalytic model to determine activation energies and reaction order. The autocatalytic model has the following form:

$$\frac{d\alpha}{dt} = k(T)\alpha^m(1-\alpha)^n \quad (3)$$

where $d\alpha/dt$ = reaction rate (1/s), k = rate constant (1/s), α = fractional conversion, and m, n = reaction orders [39,47,48]. This approach requires three or more isothermal experiments to generate the kinetic parameters (E_a, Z, n, m, and k). Table 2 summarizes the average ΔHs, activation energies and reaction orders for the neat resin and nanocomposites determined using the autocatalytic model. The ΔHs of the nanocomposites are lower than those for the neat resin; this has also been observed by others [34,37–39,49,50]. One reason for this may be that the presence of the nanotubes causes an increase in viscosity which lowers the mobility of the reactive species and results in a lower ΔH. Variations in the concentration of reactive groups on the nanotube surface can also lead to differences in resin/curing agent stoichiometry [34,35]. The activation energy of the neat and F–MWNT/EPON system is essentially the same (47.5 and 47.7 kJ/mol), while that for the COOH–MWNT/EPON system is higher (61.7 kJ/mol). This suggests that cure mechanisms of the neat resin and resin plus fluorinated nanotubes are similar, while that for the carboxylated nanotubes differs.

This suggestion is corroborated by the respective reaction mechanisms involved. A schematic of modified CNTs/polymer

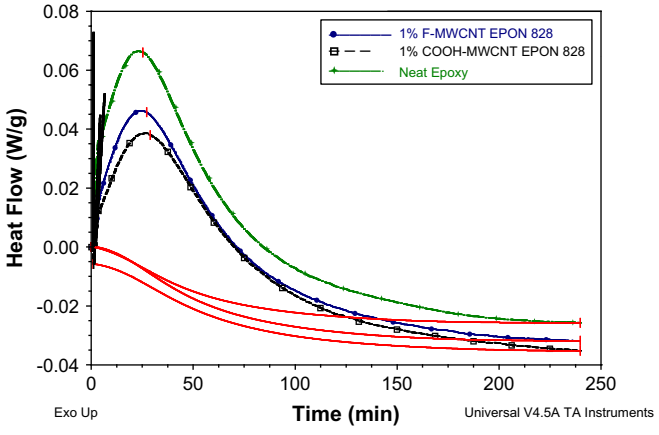

Fig. 2. Isothermal DSC thermograms at 120 °C for neat EPON828, 1% F–MWCNT/EPON828 and COOH–MWCNT/EPON828 nanocomposite.

Table 1
Enthalpy change (Δ*H*) and peak onset at inflection of neat resin and 1% nanocomposite samples from isothermal DSC scans

Sample	Enthalpy change (Δ*H*), J/g			Peak onset at inflection, min		
	$\Delta H_{Iso\ 110^\circ C}$	$\Delta H_{Iso\ 120^\circ C}$	$\Delta H_{Iso\ 140^\circ C}$	$t_{Iso\ 110^\circ C}$	$t_{Iso\ 120^\circ C}$	$t_{Iso\ 140^\circ C}$
Neat epoxy	263.4	298.3	397.0	42.9	25.3	10.8
1% COOH–MWCNT/EPON828	177.8	234.0	307.6	50.9	28.9	10.4
1% F–MWCNT/EPON828	245.6	228.5	315.91	45.4	27.1	12.4

Table 2
Activation energies and reaction order factors for the neat resin and nanocomposite systems

Sample	Average (Δ*H*), J/g	E_a, kJ/mol	*n*	*m*
Neat epoxy	319.6	47.5	1.28	0.41
1.0% COOH–MWCNT/EPON828	239.8	61.7	1.34	0.48
1.0% F–MWCNT/EPON828	263.4	47.7	1.36	0.47

Table 3
Rate constants for the neat resin and nanocomposite systems at different temperatures

Sample	Rate constant, min^{-1}		
	$T_{Iso\ 110^\circ C}$	$T_{Iso\ 120^\circ C}$	$T_{Iso\ 140^\circ C}$
Neat epoxy	0.0250	0.0428	0.0488
1.0% COOH–MWCNT/EPON828	0.0258	0.0390	0.0693
1.0% F–MWCNT/EPON828	0.0268	0.0428	0.0701

chemical interactions is shown in Fig. 3. There is a distinct difference in how the modified CNTs react with the epoxy system (i.e. resin and curing agent). The carboxyl groups on the CNT surface participate in an opening of the epoxide rings, resulting in the formation of an ester bond and an OH group [15,39]. The fluorinated CNT first undergoes a displacement reaction with the amine curing agent. Stevens et al. demonstrated that fluorine on the sidewalls of fluorinated CNT can be displaced by alkylidene amino groups at moderate temperature [9,51,52]. They suggested that the fluorinated CNT may also react in situ with the amine curing agents during a high temperature curing process of the epoxy systems. This results in an amine modified CNT which can essentially act as a curing agent and react with other epoxy groups.

The relative rate constants (Table 3) for the nanocomposite samples are similar to those of the neat resin at 110 °C. At 122 °C the value of the rate constants for the neat resin and the fluorinated system is the same, while that for the COOH–MWNT/EPON system is slightly lower. At 140 °C, the values for the nanocomposites are similar, while that of the neat resin is lower. The differences in the value of the rate constants may be correlated with the CNT dispersion. In the fluorinated system, the CNTs are well dispersed, allowing more surface area to be in contact with the resin. As a result, the high thermal conductivity and surface area of the CNTs enhance the rate of the curing reaction [38]. The presence of aggregates in the more poorly dispersed COOH–MWNT/EPON system results in less surface area in contact with resin and hence less of a catalytic effect [39]. At a higher temperature of 140 °C, differences in rates of the nanocomposites are indistinguishable.

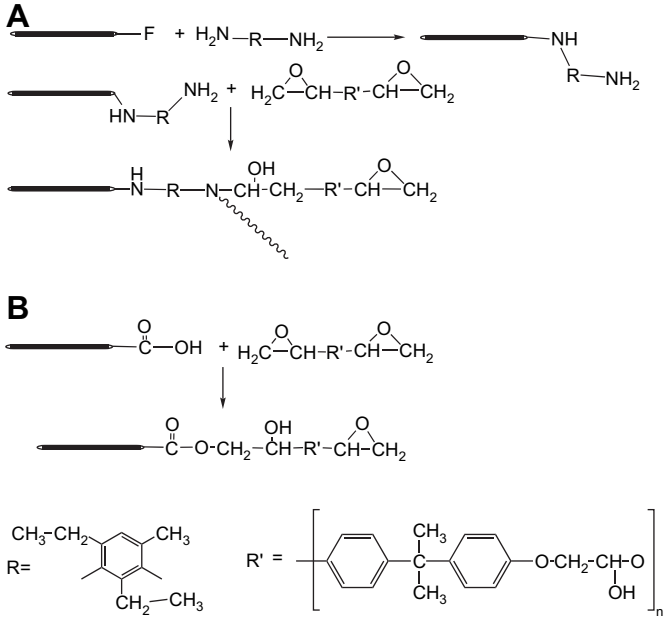

Fig. 3. Reaction scheme for modified CNT reaction with DGEBA resin. (A) Fluorinated CNT reaction with curing agent and DGEBA. (B) Carboxylated CNT reaction with DGEBA resin.

3.2. Heat capacity and rheological measurements of curing process

The evolution of the storage modulus (G') during cure for the neat resin, and nanocomposites with 1 wt% of fluorine and carboxylated modified CNTs is shown in Fig. 4. In general, induction times ranging from 2500 to approximately 4000 s are observed before a rapid increase in modulus occurs. The storage modulus is highest for the fluorinated system during the induction period. Since the storage modulus is a measure of the stiffness of the prepolymer, presumably the mechanical differences are related to variations in the aspect ratio, which would lead to variations in load transfer and stiffness. This is plausible when the methods of surface modification are considered. The fluorination modification method is not as harsh as the oxidation method used to prepare the carboxyl-modified CNTs, which involves exposing the nanotubes to a mixture of sulfuric and nitric acid. This can actually cut the nanotubes and also create defects in the wall surface [35]. As

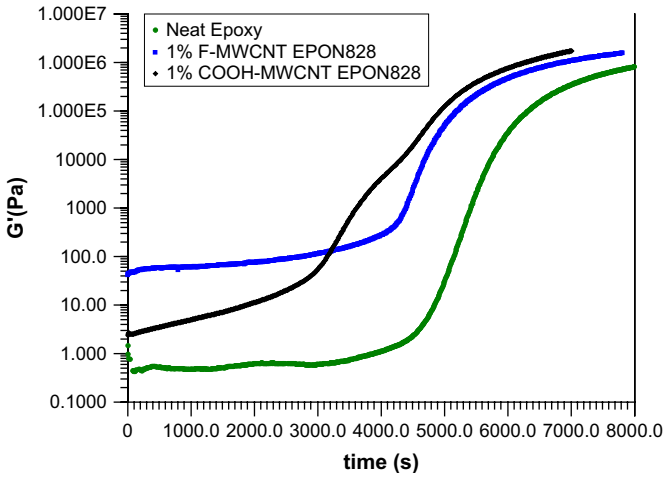

Fig. 4. Isothermal cure behavior of neat epoxy resin and nanocomposites at 120 °C.

a result the fluorinated nanotubes have fewer structural defects and a higher aspect ratio. The gel points for these systems, taken as the point at which the storage and loss moduli (not shown in this plot) cross, are summarized in Table 4. The gelation is fastest for the COOH–MWNT/EPON (58 min), while the neat resin and fluorinated systems have gel times of 81 and 78 min, respectively.

The shape of the curve for the fluorinated system is also similar to that for the neat resin, while the curve for the carboxyl system is distinctly different, with a shoulder observable. Ganguli et al. also observed shoulders in dynamic mechanical relaxation data for cyanate ester/layered silicates and they attributed this to a heterogeneous crosslink topology, caused by partitioning of the reactive species by the silicates [53]. We suggest that a similar effect is occurring in our samples.

Studies of the molecular mobility during the cure process, using heat capacity and rheological behavior, were used to gain more insight into how the interfacial chemistry affects the cure mechanisms involved. In addition to changes in heat flow during isothermal cure, heat capacity changes can provide additional insight on the cure behavior. Vitrification times at 120 °C were determined from plots of C_p vs. time, by determining the onsets of the C_p decrease. The heat capacity is related to the molecular mobility, with a higher mobility corresponding to a larger value of C_p [48]. Fig. 5 plots the C_p as a function of time for the neat resin and nanocomposites at 120 °C. Similar changes in C_p were observed at the other isothermal temperatures. The COOH–MWNT/EPON system exhibits the highest C_p, followed by the neat resin and fluorinated system. Significant changes in C_p typically occur during the final stage (crosslinking) of cure.

Table 4
Gel points of the neat resin and CNT/EPON828 nanocomposite systems

Sample	Gel point time, min
Neat epoxy	81.4
1.0% COOH–MWCNT/EPON828	58
1.0% F–MWCNT/EPON828	78.5

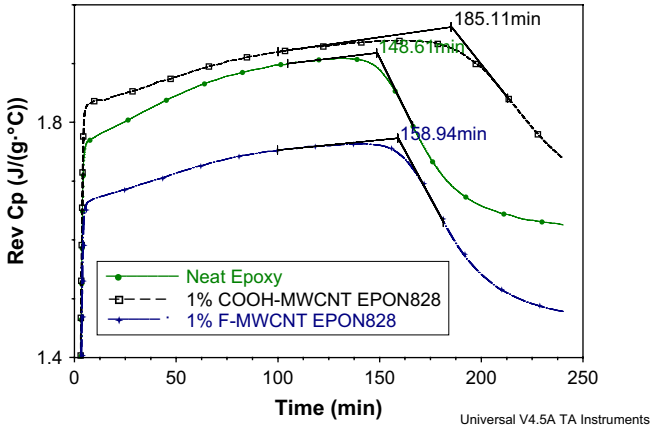

Fig. 5. Reverse heat capacity from quasi-isothermal scan at 120 °C for the neat resin and nanocomposite system.

As curing progresses to the final stages, the curves exhibit a significant decrease associated with the onset of vitrification. The neat sample has the shortest onset time (150 min), followed by the fluorinated system (161 min) and the carboxylated system (190 min). The neat resin vitrifies more quickly, presumably since there are no CNTs present to interfere with the mobility of the reacting species. Although the carboxylated system gels faster, it takes longer to vitrify. Since C_p is related to molecular mobility, presumably a more heterogeneous dispersion of the CNTs in the carboxylated system retards the mobility of the reacting species, resulting in a longer vitrification time. This can be seen in high resolution scanning electron microscopic images, Fig. 6, which show that the CNTs are very well dispersed in the fluorinated system (denoted by the white features inside the red circle on the micrograph), whereas the dispersion of carboxyl-modified CNTs is not so good. (For interpretation of the references to colour in this text, the reader is referred to the web version of this article.)

When the findings from the thermal and rheological experiments are combined, we can paint a picture of the curing process and how it is affected by the nanotube surface chemistry. During isothermal cure, the neat resin begins to cure first, as shown by its shorter onset time in DSC experiments. As the reaction proceeds, the enthalpy of reaction decreases for the nanocomposites, with the largest decrease observed for the carboxylated sample (Table 2). The rate constants, gel points and vitrification times for the neat resin and the fluorinated sample are relatively close, while those for the carboxylic acid sample are significantly different. This suggests that the cure mechanisms for the neat and fluorinated samples are similar. This is corroborated by the chemistry of the nanotube–epoxy reaction depicted in Fig. 1. Once the fluorinated nanotubes undergo an exchange reaction with the amines, they react with the epoxy resin in a manner similar to that of the amine curing agent.

3.3. Degree of conversion

3.3.1. Differential scanning calorimetry

Differences in the ΔHs observed for the nanocomposites seem to suggest that the CNTs are preventing the epoxy resin from attaining a degree of cure similar to that of the neat resin; thus Eq. (3) was

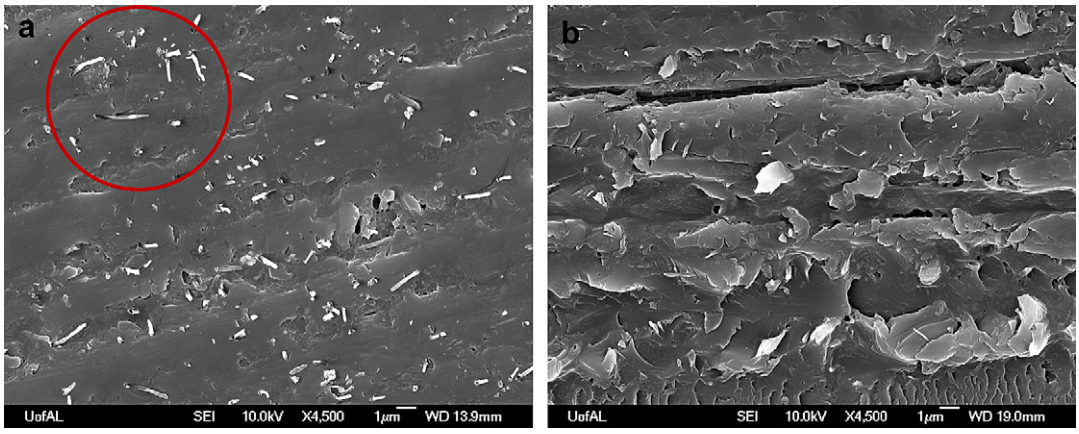

Fig. 6. SEM images of (a) F–MWCNT/EPON828 and (b) COOH–MWCNT/EPON828 nanocomposite.

used to predict the degree of conversion α for the three samples vs. time at 120 °C, using the heat flow measured during the isothermal cure. The result is shown in Fig. 7. Similar plots for each sample can be obtained at the other isothermal temperatures. For a given temperature the plots show a steeper slope or faster reaction rate in the initial stage when the concentrations of reactive species are the highest, after which the reaction conversion passes through a maximum before it starts to slow down, a phenomenon usually observed in autocatalytic curing reactions. The neat resin and F–MWCNT/EPON828 have very similar conversion rates, with a slightly different rate for the COOH–MWCNT/EPON828 nanocomposite. As the reaction proceeds, the latter stages become diffusion controlled, and the mobility of the reacting species decreases significantly until the reaction ceases. As a result, the conversion never reaches 100%, and this is seen in the data in Fig. 7.

A plot of $\ln(1-\alpha)$ vs. time, shown in Fig. 8, shows that the curing reaction is not a simple first order reaction which is consistent with the reaction orders shown in Table 2. The slope change at approximately 2 h indicates the reaction shifts from kinetic control to diffusion control. Curing kinetics of thermosets are known to follow initially first order reaction, followed by deviation at the onset of diffusion control, caused by vitrification [54].

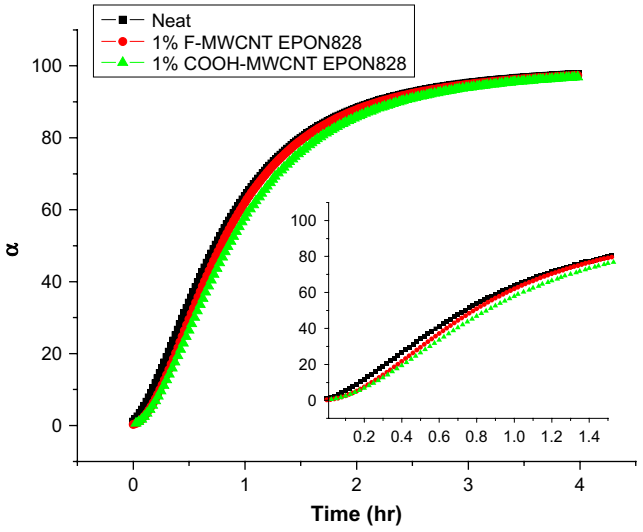

Fig. 7. Comparison of conversion percent of the neat resin and the nanocomposite system from DSC (the inset shows the change of the slope for the first hour).

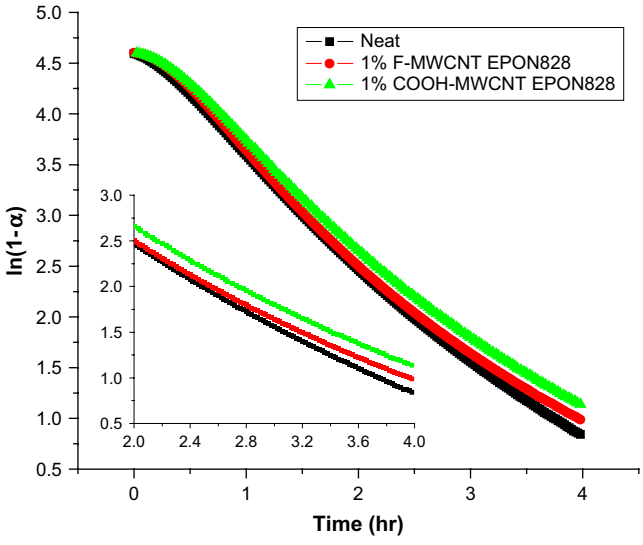

Fig. 8. Plot of $\ln(1-\alpha)$ vs. time for the neat resin and the nanocomposite system (the inset shows the change of the slope for the last 2 h).

3.3.2. FT-IR

The degree of conversion of the epoxy resins was also measured by taking an IR scan after they were cured. This degree of cure, or conversion percent, was calculated using the following equation:

$$\alpha = 1 - \frac{A_{t=x}}{A_{t=0}} \tag{4}$$

where $A_{t=x}$ is the area of the epoxide peak at time x, $A_{t=0}$ is the area of the uncured epoxide peak, which would be visible at 911 cm^{-1}. The result from the IR data, shown in Table 5, showed a very good agreement with the predictions based on DSC data shown in Fig. 7. Further confirmation is provided by the T_gs determined from dynamic DSC scans, shown in Fig. 9, and listed in Table 5. The T_g is a very sensitive indicator of the degree of conversion in a thermoset polymer. The T_g typically increases as the reaction proceeds until it reaches the cure temperature. At this point the sample vitrifies and the molecular mobility decreases [55,56]. The T_g value is approximately 119 °C for all nanocomposites and neat resin samples, indicating that the samples are equally cured. This agrees with the predicted cure from the DSC data as shown in Fig. 7. In addition, examination of the DSC scans in Fig. 9, that were used to measure the T_g, did not show any residual curing. Thus the presence of modified CNTs affects the epoxy/cure agent cure mechanism, but not the overall degree of cure.

Table 5
Glass transition temperature and degree of conversion using IR of the neat resin and CNT/EPON828 nanocomposite systems

Sample	T_g, °C	Degree of conversion, %
Neat epoxy	119	95
1.0% COOH–MWCNT/EPON828	120	96
1.0% F–MWCNT/EPON828	119	96

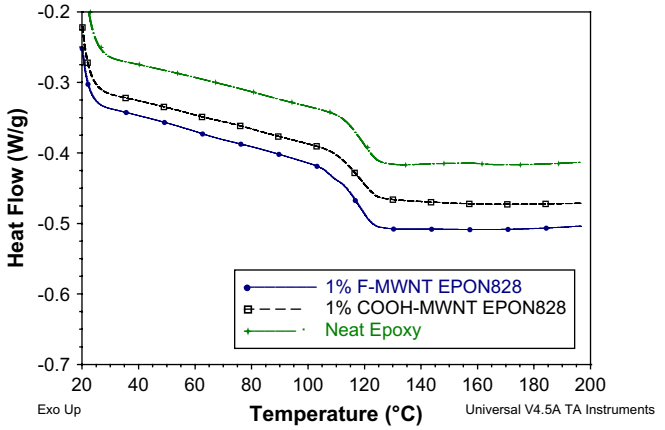

Fig. 9. Dynamic DSC thermograms for cured neat EPON828 and nanocomposite samples.

4. Conclusion

In this work, we studied the effect of carboxylated and fluorinated multi-wall CNTs on the cure behavior of diglycidyl ether of bisphenol A epoxy resin using differential scanning calorimetry, rheology and infrared spectroscopy.

Investigation of isothermal curing using rheology, FT-IR and heat capacities from modulated DSC help to elucidate differences in the cure behavior caused by the CNT surface chemistry. During

isothermal cure, the neat resin begins to cure first, as shown by its shorter onset time, measured by DSC. As the reaction proceeds, the enthalpy of reaction decreases for the nanocomposites, with the largest decrease observed for the carboxyl-modified sample. As curing progresses, the gel points for the neat resin and the fluorinated sample are relatively close, while that for the carboxyl-modified sample is significantly faster. As the samples vitrify and the reaction is completed, the neat resin vitrifies first, followed by the fluorinated and finally the carboxyl sample.

Comparison of the activation energies, rate constants, gelation behavior and vitrification times suggests that the cure mechanisms of the neat resin and fluorinated sample are similar but different from the carboxylated sample. This can be explained by the difference in how the fluorinated nanotubes react with the epoxy compared to the carboxylated nanotubes. In addition to differences in reaction mechanism, variation in nanotube dispersion can also have an effect on the cure behavior. The fluorinated MWCNT system is more uniformly dispersed in the matrix whereas the more heterogeneously dispersed carboxylated MWCNTs can hinder the mobility of the reactive species, disrupting the reaction stoichiometry on the local scale and altering the cure kinetics. The concentration of functional groups on the CNTs' surface can also play a role in altering the dispersion and the cure behavior. Although the two systems have different reaction mechanisms, both systems have similar degrees of conversion as calculated from the IR data, glass transition temperature and predictions based on DSC data.

Acknowledgement

This work was funded by NSF DMR (Grant 0404278).

References

[1] Moniruzzaman M, Winey KI. Polymer nanocomposites containing carbon nanotubes. Macromolecules 2006;39(16):5194–205.
[2] Xie X, Mai Y, Zhou X. Dispersion and alignment of carbon nanotubes in polymer matrix: a review. Mater Sci Eng R Rep 2005;49(4):89–112.
[3] Belin T, Epron F. Characterization methods of carbon nanotubes: a review. Mater Sci Eng B 2005;119(2):105–18.
[4] Thostenson ET, Ren Z, Chou T. Advances in the science and technology of carbon nanotubes and their composites: a review. Compos Sci Technol 2001; 61(13):1899–912.
[5] Coleman JN, Khan U, Gun'ko YK. Mechanical reinforcement of polymers using carbon nanotubes. Adv Mater 2006;18(6):689–706.
[6] Lau K, Chipara M, Ling H, Hui D. On the effective elastic moduli of carbon nanotubes for nanocomposite structures. Composites Part B Eng 2004;35(2): 95–101.
[7] Camponeschi E, Florkowski B, Vance R, Garrett G, Garmestani H, Tannenbaum R. Uniform directional alignment of single-walled carbon nanotubes in viscous polymer flow. Langmuir 2006;22(4):1858–62.
[8] Park C, Ounaies Z, Watson KA, Crooks RE, Smith J Joseph, Lowther SE, et al. Dispersion of single wall carbon nanotubes by in situ polymerization under sonication. Chem Phys Lett 2002;364(3–4):303–8.
[9] Zhu J, Kim J, Peng H, Margrave JL, Khabashesku VN, Barrera EV. Improving the dispersion and integration of single-walled carbon nanotubes in epoxy composites through functionalization. Nano Lett 2003;3(8):1107–13.
[10] Du F, Scogna RC, Zhou W, Brand S, Fischer JE, Winey KI. Nanotube networks in polymer nanocomposites: rheology and electrical conductivity. Macromolecules 2004;37(24):9048–55.
[11] Choi ES, Brooks JS, Eaton DL, Al-Haik MS, Hussaini MY, Garmestani H, et al. Enhancement of thermal and electrical properties of carbon nanotube polymer composites by magnetic field processing. J Appl Phys 2003;94(9): 6034–9.
[12] Gojny FH, Wichmann MHG, Kopke U, Fiedler B, Schulte K. Carbon nanotube-reinforced epoxy-composites: enhanced stiffness and fracture toughness at low nanotube content. Compos Sci Technol 2004;64(15):2363–71.
[13] Ganguli S, Bhuyan M, Allie L, Aglan H. Effect of multi-walled carbon nanotube reinforcement on the fracture behavior of a tetrafunctional epoxy. J Mater Sci 2005;40(13):3593–5.
[14] Liao Y, Marietta-Tondin O, Liang Z, Zhang C, Wang B. Investigation of the dispersion process of SWNTs/SC-15 epoxy resin nanocomposites. Mater Sci Eng A 2004;385(1–2):175–81.
[15] Eitan A, Jiang K, Dukes D, Andrews R, Schadler LS. Surface modification of multiwalled carbon nanotubes: toward the tailoring of the interface in polymer composites. Chem Mater 2003;15(16):3198–201.
[16] Breton Y, Delpeux S, Benoit R, Sallvetat J, Sinturel C, Beguin F. Functionalization of multiwall carbon nanotubes properties of nanotubes–epoxy composites. Mol Cryst Liq Cryst 2002;387:135–40.
[17] Breton Y, Desarmot G, Salvetat JP, Delpeux S, Sinturel C, Beguin F, et al. Mechanical properties of multiwall carbon nanotubes/epoxy composites: influence of network morphology. Carbon 2004;42(5–6):1027–30.
[18] Song YS, Youn JR. Influence of dispersion states of carbon nanotubes on physical properties of epoxy nanocomposites. Carbon 2005;43(7):1378–85.
[19] Miyagawa H, Mohanty AK, Drzal LT, Misra M. Nanocomposites from biobased epoxy and single-wall carbon nanotubes: synthesis, and mechanical and thermophysical properties evaluation. Nanotechnology 2005;1:118–24.
[20] Lau K, Lu M, Lam C, Cheung H, Sheng F, Li H. Thermal and mechanical properties of single-walled carbon nanotube bundle-reinforced epoxy nanocomposites: the role of solvent for nanotube dispersion. Compos Sci Technol 2005;65(5):719–25.
[21] Gojny FH, Schulte K. Functionalisation effect on the thermo-mechanical behaviour of multi-wall carbon nanotube/epoxy-composites. Compos Sci Technol 2004;64(15):2303–8.
[22] Miyagawa H, Drzal LT. Thermo-physical and impact properties of epoxy nanocomposites reinforced by single-wall carbon nanotubes. Polymer 2004; 45(15):5163–70.
[23] Wang Z, Liang Z, Wang B, Zhang C, Kramer L. Processing and property investigation of single-walled carbon nanotube (SWNT) buckypaper/epoxy resin matrix nanocomposites. Composites Part A Appl Sci Manuf 2004;35(10): 1225–32.
[24] Gojny FH, Nastalczyk J, Roslaniec Z, Schulte K. Surface modified multi-walled carbon nanotubes in CNT/epoxy-composites. Chem Phys Lett 2003;370(5–6): 820–4.
[25] Sandler J, Shaffer MSP, Prasse T, Bauhofer W, Schulte K, Windle AH. Development of a dispersion process for carbon nanotubes in an epoxy matrix and the resulting electrical properties. Polymer 1999;40(21):5967–71.
[26] Sandler JKW, Kirk JE, Kinloch IA, Shaffer MSP, Windle AH. Ultra-low electrical percolation threshold in carbon-nanotube–epoxy composites. Polymer 2003; 44(19):5893–9.
[27] Schadler LS, Giannaris SC, Ajayan PM. Load transfer in carbon nanotube epoxy composites. Appl Phys Lett 1998;73(26):3842–4.
[28] Zhu J, Peng H, Rodriguez-Macias F, Margrave JL, Khabashesku VN, Imam AM, et al. Reinforcing epoxy polymer composites through covalent integration of functionalized nanotubes. Adv Funct Mater 2004;14(7):643–8.
[29] Coleman JN, Khan U, Blau WJ, Gun'ko YK. Small but strong: a review of the mechanical properties of carbon nanotube–polymer composites. Carbon 2006;44(9):1624–52.
[30] Hussain F, Hojjati M, Okamoto M, Gorga RE. Review article: polymer–matrix nanocomposites, processing, manufacturing, and application: an overview. J Compos Mater 2006;40(17):1511–75.
[31] Liu TX, Phang IY, Shen L, Chow SY, Zhang WD. Morphology and mechanical properties of multiwalled carbon nanotubes reinforced nylon-6 composites. Macromolecules 2004;37(19):7214–22.
[32] Shofner ML, Khabashesku VN, Barrera EV. Processing and mechanical properties of fluorinated single-wall carbon nanotube–polyethylene composites. Chem Mater 2006;18(4):906–13.
[33] Liu L, Wagner HD. Rubbery and glassy epoxy resins reinforced with carbon nanotubes. Compos Sci Technol 2005;65(11–12):1861–8.
[34] Wang S, Liang Z, Liu T, Wang B, Zhang C. Effective amino-functionalization of carbon nanotubes for reinforcing epoxy polymer composites. Nanotechnology 2006;17(6):1551–7.
[35] Abdalla M, Dean D, Adibempe D, Nyairo E, Robinson P, Thompson G. The effect of interfacial chemistry on molecular mobility and morphology of multiwalled carbon nanotubes epoxy nanocomposite. Polymer 2007;48(19): 5662–70.
[36] Sandler JKW, Windle AH, Martin CA, Schwarz M-K, Bauhofer W, Schulte K, et al. Percolation in multi-wall carbon nanotube–epoxy composites influence of processing parameters, nanotube aspect ratio and electric fields on the bulk conductivity. Boston, MA, United States: Materials Research Society; 2003.
[37] Puglia D, Valentini L, Armentano I, Kenny JM. Effects of single-walled carbon nanotube incorporation on the cure reaction of epoxy resin and its detection by Raman spectroscopy. Diamond Relat Mater 2003;12(3–7):827–32.
[38] Puglia D, Valentini L, Kenny JM. Analysis of the cure reaction of carbon nanotubes/epoxy resin composites through thermal analysis and Raman spectroscopy. J Appl Polym Sci 2003;88(2):452–8.
[39] Tao K, Yang S, Grunlan JC, Kim Y-S, Dang B, Deng Y, et al. Effects of carbon nanotube fillers on the curing processes of epoxy resin-based composites. J Appl Polym Sci 2006;102(6):5248–54.
[40] Borchardt HJ, Daniels F. The application of differential thermal analysis to the study of reaction kinetics. J Am Chem Soc 1957;79(1):41–6.
[41] Swarin SJ, Wims AM. A method for determining reaction kinetics by differential scanning calorimetry. J Therm Anal Calorim 1976;4(155).
[42] Kenny JM, Trivisano A. Isothermal and dynamic reaction kinetics of high performance epoxy matrices. Polym Eng Sci 1991;31(19):1426–33.
[43] Kenny JM. Determination of autocatalytic kinetic model parameters describing thermoset cure. J Appl Polym Sci 1994;51(4):761–4.
[44] Peyser P, Bascom WD. Comments on the paper (1) "analysis of curing kinetics in polymer composites". J Appl Polym Sci 1975;13(3):129–30.
[45] Peyser P, Bascom WD. Kinetics of epoxy resin polymerization using differential scanning calorimetry. J Appl Polym Sci 1977;21(9):2359–73.

[46] Xie H, Liu B, Yuan Z, Shen J, Cheng R. Cure kinetics of carbon nanotube/tetrafunctional epoxy nanocomposites by isothermal differential scanning calorimetry. J Polym Sci Part B Polym Phys 2004;42(20):3701–12.
[47] Keenan MR. Autocatalytic cure kinetics from DSC measurements: zero initial cure rate. J Appl Polym Sci 1987;33(5):1725–34.
[48] Patel RD, Patel RG, Patel VS, Pearce EM. Kinetic investigation on the curing of phenol- furfural resin by differential scanning calorimetry. J Appl Polym Sci 1987;34(7):2583–9.
[49] Bae J, Jang J, Yoon S-H. Cure behavior of the liquid-crystalline epoxy/carbon nanotube system and the effect of surface treatment of carbon fillers on cure reaction. 2002:2196–204.
[50] Valentini L, Armentano I, Puglia D, Kenny JM. Dynamics of amine functionalized nanotubes/epoxy composites by dielectric relaxation spectroscopy. Carbon 2004;42(2):323–9.
[51] Stevens JL, Huang AY, Peng H, Chiang IW, Khabashesku VN, Margrave JL. Sidewall amino-functionalization of single-walled carbon nanotubes through fluorination and subsequent reactions with terminal diamines. Nano Lett 2003;3(3):331–6.
[52] Smith MB. Organic synthesis. 2nd ed. New York: McGraw-Hill; 1946.
[53] Ganguli S, Dean D, Jordan K, Price G, Vaia R. Mechanical properties of intercalated cyanate ester-layered silicate nanocomposites. Polymer 2003;44(4):1315–9.
[54] Ganguli S, Dean D, Jordan K, Price G, Vaia R. Chemorheology of cyanate ester-organically layered silicate nanocomposites. Polymer 2003;44(22):6901–11.
[55] Rozenberg BA. Kinetics, thermodynamics and mechanism of reactions of epoxy oligomers with amines. Adv Polym Sci 1986;75:113–65.
[56] Oleinik E. Epoxy–aromatic amine networks in the glassy state structure and properties, Epoxy resins and composites IV; 1980. p. 49–99.